

## High-nickel layered oxide cathodes for lithium-based automotive batteries

Wangda Li, Evan M. Erickson, and Arumugam Manthiram\*

Materials Science and Engineering Program and Texas Materials Institute, University of Texas at Austin, Austin, Texas 78712, USA

\*Corresponding author: [manth@austin.utexas.edu](mailto:manth@austin.utexas.edu)

High-nickel layered oxide cathode materials will be at the forefront to enable longer driving-range electric vehicles at more affordable costs with lithium-based batteries. A continued push to higher energy content and less usage of costly raw materials, such as cobalt, while preserving acceptable power, lifetime, and safety metrics, calls for a suite of strategic compositional, morphological, and microstructural designs and efficient material production processes. In this Perspective, we discuss several important design considerations for high-nickel layered oxide cathodes that will be implemented in the automotive market for the coming decade. We outline various intrinsic restraints of maximizing their energy output and compare current/emerging development roadmaps approaching low-/zero-cobalt chemistry. Materials production is another focus, relevant to driving down costs and addressing the practical challenges of high-nickel layered oxides for demanding vehicle applications. We further assess a series of stabilization techniques on their prospects to fulfill the aggressive targets of vehicle electrification.

Electric mobility is rapidly expanding. In 2018, the global fleet of plug-in hybrid electric vehicles (PHEVs) and battery-electric vehicles (BEVs) reached 5.4 million, up 2.1 million from the previous year<sup>1</sup>. Among owners of electric vehicles (EVs), ‘range anxiety’ is still a primary concern, including limited driving range, lack of sufficient charging facilities, and severe range loss at cold climates. Compared with representative internal combustion engine (ICE) vehicles of varying prices, latest BEVs fall short across the board (**Table 1**). While some luxury models can travel up to 600 km on a single charge, affordable BEVs (*e.g.*, ≤ 30,000 US\$) are still far from providing consumers the range performance of conventional vehicles. Nevertheless, recent dynamic developments in electromobility, from technological advances in battery chemistry and vehicle manufacturing platforms, to policy support such as stricter fuel economy standards and incentives for low-/zero-emission vehicles, as well as ambitious private sector investment to ramp up production and expand charging infrastructure, will further open the floodgates of demand and underpin a positive outlook for electrification of transportation across the globe (**Fig. 1a**)<sup>2</sup>.

Lithium-ion batteries (LIBs), the current sole power source for EV propulsion, show up to 150–170 Wh kg<sup>-1</sup> (ref. 3,4) with a volume-averaged price of 176 US\$ kWh<sup>-1</sup> (ref. 5) at the pack level. To enable the full driving performance and price of an ICE vehicle, the U.S. Department of Energy estimated that automotive batteries need to deliver 235 Wh kg<sup>-1</sup>/500 Wh l<sup>-1</sup> at 100 US\$ kWh<sup>-1</sup> at pack level (350 Wh kg<sup>-1</sup>/750 Wh l<sup>-1</sup> at 75 US\$ kWh<sup>-1</sup> at cell level)<sup>6</sup>. Besides assembly, control and cooling systems of battery packs and powertrain modules, higher energy output and cost savings will directly come from cell chemistry<sup>7,8</sup>. Over the last decade, nickel-based layered oxides, *e.g.*, Li[Ni<sub>a</sub>Co<sub>b</sub>Mn<sub>c</sub>]O<sub>2</sub> ( $a+b+c = 1$ ; NCM-*abc*) and Li[Ni<sub>1-x-y</sub>Co<sub>x</sub>Al<sub>y</sub>]O<sub>2</sub> (NCA), solidified their status as the cathode material of choice for passenger EV batteries while gradually phasing out cubic spinel LiMn<sub>2</sub>O<sub>4</sub> (LMO) and olivine LiFePO<sub>4</sub>

(LFP) (**Table 1** and **Fig. 1c**). The 300 Wh kg<sup>-1</sup> cell-level energy milestone was lately achieved, *e.g.*, CATL (NCM-811, pouch format) and Panasonic (NCA, 21700 cylindrical format). State-of-the-art LFP, however, only shows up to 180–190 Wh kg<sup>-1</sup><sub>cell</sub> despite a lower price of 80–135 US\$ kWh<sup>-1</sup><sub>cell</sub> (ref. 9), *vs.* 100–175 US\$ kWh<sup>-1</sup><sub>cell</sub> for NCM/NCA. In China, NCM/NCA took up nearly 90% of installed battery capacity for passenger EVs in 2018 (33.1 GWh), a further leap from 72% in 2017 (ref. 3,10). On the other hand, LFP still dominates in commercial EVs (23.8 GWh) and provides unmatched total energy throughput, capable of 600,000–800,000 km accumulated driving distance<sup>9</sup>.

A cell-level specific energy of 350 Wh kg<sup>-1</sup> with next-generation layered oxide cathodes (**Fig. 1c**) and graphite-silicon anodes is expected by 2025 or sooner<sup>3</sup>. The cathode, normally the largest component by both weight and cost in state-of-the-art LIB cells<sup>3,8,11</sup>, is still a main bottleneck (an example in **Fig. 1b**). As driving range requirements impose higher energy content nearing fundamental limits of layered oxides, challenges arise to maintain a delicate balance among other key parameters, *i.e.*, power, lifetime, safety, and cost. Successful designs will rely on a game of trade-offs – fine tuning of composition, morphology, microstructure, and surface properties of the active material, as well as thickness/porosity of the composite electrode<sup>12,13</sup>. Meanwhile, the raw material costs in NCM/NCA could be an obstacle, with limited cobalt supplies (**Fig. 1e**) subject to political instabilities in Central Africa<sup>11,14</sup>. Lithium and nickel are abundant<sup>14</sup>, but mining projects suitable for battery applications need time to develop<sup>2</sup>.

This Perspective discusses several key considerations for designing next-generation nickel-based layered oxide cathodes, from laboratory screening to industrial production. We survey critical intrinsic and practical issues associated with the current push to higher energy

content and low-/zero-cobalt usage. Another focus is the material production processes relevant at the large scale. An outlook for future developments is also given.

### Compositional design principles

To enable a cell-level specific energy of  $\geq 350 \text{ Wh kg}^{-1}$ , it is estimated that at least  $800 \text{ Wh kg}^{-1}$  is needed from the cathode active material based on the chemistry and design of state-of-the-art LIBs<sup>8,12</sup> (*e.g.*, no Li metal anode; **Fig. 1d**). In the meantime, higher energy content would ideally come from chemical formulations with little or no cobalt. Here, we discuss several important compositional design considerations of next-generation nickel-based layered oxides to approach these targets.

**High nickel vs. high voltage.** A general approach to increase the energy output in layered oxide cathodes is through an increase in the nickel content<sup>12</sup>. At  $4.3 \text{ V}_{\text{Li}}$ , roughly  $200 \text{ mAh g}^{-1}$  specific capacity can be reversibly accessed from NCM-811 ( $\text{LiNi}_{0.8}\text{Co}_{0.1}\text{Mn}_{0.1}\text{O}_2$ ) and NCA-80 ( $\text{LiNi}_{0.8}\text{Co}_{0.15}\text{Al}_{0.05}\text{O}_2$ ), in comparison to  $160 \text{ mAh g}^{-1}$  from NCM-111 ( $\text{LiNi}_{1/3}\text{Co}_{1/3}\text{Mn}_{1/3}\text{O}_2$ ). In actuality, by virtue of much less oxygen loss than from  $\text{LiCoO}_2$  at highly delithiated states, NCM/NCA across the entire composition spectrum can reach  $800 \text{ Wh kg}^{-1}_{\text{cathode}}$  (or  $210\text{--}215 \text{ mAh g}^{-1}$  at  $3.7\text{--}3.8 \text{ V}_{\text{Li}}$ ) while maintaining structural integrity at sufficiently high charging voltages<sup>15</sup> (**Fig. 2**). **Table 2** compares two extreme cases for pushing the Ni content or upper cut-off voltage (*i.e.*, ‘ultrahigh nickel’, **Fig. 2b** and ‘ultrahigh voltage’, **Fig. 2c**), respectively, relative to commercial layered oxides.

The main challenges with a large degree of Li utilization in layered oxides are substantially compromised cycle and thermal stability. Irrespective of the nickel fraction, all compositions undergo singlet oxygen evolution (electrolyte oxidation)<sup>16</sup>, transition-metal dissolution<sup>17</sup>, rock-salt phase formation<sup>18</sup>, and anisotropic lattice distortion (particle cracking)<sup>15</sup> (**Fig. 2d-2h**).

The ‘ultrahigh voltage’ route brings marginal advantages in thermal-abuse tolerance<sup>19</sup>, but faces compatibility issues of electrolytes (**Fig. 2i**) and a supply risk of cobalt. In the ‘ultrahigh nickel’ case, additional problems include multistep two-phase reactions during (de)lithiation (particle cracking)<sup>20</sup> and surface residual Li compounds (storage issues<sup>21</sup> and gas evolution from electrolyte reactivity<sup>22</sup>, **Fig. 2j**). Besides the above concerns, the ‘ultrahigh nickel’ case enjoys superior energy efficiency and rate capability, but requires more complex synthesis and conditioning processes<sup>23,24</sup> and lower electrode density to ensure cyclability (see below for more details)<sup>13</sup>.

In the last decade, increases in the energy content of NCM for automotive batteries have been predominantly powered through higher Ni incorporation (*i.e.*, the progression of NCM-111→NCM-523→NCM-622→NCM-811). NCA, initially with high Ni content (*e.g.*, NCA-80), saw only a modest increase from  $\sim 250 \text{ Wh kg}^{-1}_{\text{cell}}$  in 2009<sup>25</sup>. This trend testifies to the sheer practical difficulties of extending operating voltages of NCM/NCA. Weighing the various aspects in **Table 2**, future generations of high-energy layered oxides will reside in between the two extreme cases. The optimally combined Ni fraction and operating voltages to reach  $\geq 800 \text{ Wh kg}^{-1}_{\text{cathode}}$  depend on further development in the field not limited to the cathode material alone (*e.g.*, high-voltage electrolytes<sup>26</sup>, cell housing materials<sup>8</sup>) and different market needs on energy throughput, power, safety, and cost<sup>7</sup>. It is worth noting that higher-Ni layered oxides do not necessarily possess fundamentally inferior electrochemical stability to their lower-Ni counterparts. Rather, the degree of lithium utilization, contrary to popular conceptions, is often the deciding parameter.

**Low cobalt.** Besides energy content, there is currently an incentive to lessen the dependence on cobalt of automotive batteries. A scarce, costly metal primarily mined from Central Africa<sup>14</sup>, demand for cobalt could outstrip supply with surging global EV production,

projected to multiply by tenfold from 2018 in the coming decade (**Fig. 1a**)<sup>2</sup>. State-of-the-art NCM uses 80–200 g of Co and 500–650 g of Ni per kWh. Current supplies of Co, Li, and Ni stand at roughly 120,000, 250,000, and 2,000,000 metric tons per annum, respectively (**Fig. 1e**). In 2025, Umicore estimated that 90,000, 375,000, and 300,000 tons of these metals are needed for rechargeable batteries<sup>27</sup>. Unlike Co, development of Li mining is far easier owing to the abundance and a more even geographical distribution of global Li reserves (Australia, Latin America, and China)<sup>14</sup>. Moreover, > 95% of world's Li is produced as a primary product in brines and hardrock ores, while Co is predominantly a by-product of Cu/Ni mines. To sustain the rapid expansion of electric mobility, layered oxides should contain a Co content no greater than, *e.g.*, 50 g per kWh<sup>28</sup>. In such a case, the annual demand for Co, Li, and Ni is projected to exceed 120,000, 1,000,000, and 1,100,000 metric tons, respectively, by 2030<sup>27</sup>. The supplies of Ni, albeit abundant through at least the next decade, will need to expand the Class I purity ( $\geq 99.8\%$ ) segment suitable for battery applications<sup>2,27</sup>.

To reduce the cobalt usage, one must first consider its essential roles along with those of manganese and aluminum in nickel-based layered oxides (**Fig. 2k**). Co and Al enhance rate capability by reducing  $\text{Li}^+/\text{Ni}^{2+}$  mixing, and for high-Ni NCM/NCA, mitigate the formation of surface residual Li compounds<sup>21,29,30</sup>. The incorporation of Mn and Al in NCM and NCA, respectively, is critical to cycle and thermal stability through suppressing multistep two-phase reactions and stabilizing the layered structure during de(lithiation)<sup>31-33</sup>. To this end, 5% Al is empirically sufficient whereas  $\geq 20\%$  Mn is generally required. The main limitations of Al doping are structural rigidity during cycling (particle cracking)<sup>34,35</sup>, a narrow solubility range without impurity phases<sup>36</sup>, and more complex synthesis<sup>23</sup>. Mn, on the other hand, despite a very low cost and facile synthesis, deteriorates rate capability by promoting more  $\text{Li}^+/\text{Ni}^{2+}$  mixing<sup>37</sup>.

Of late, state-of-the-art NCA with < 50 g Co per kWh from Panasonic has already been deployed in Tesla Model 3 batteries<sup>38</sup>, and the rollout of zero-Co chemistry is anticipated<sup>39</sup>. Meanwhile, commercialization of NCM-811 (80–100 g Co per kWh) has been bumpy due to stability issues during battery operation. After multiple delays, the first mass-produced EV carrying NCM-811 has been delivered in 2019 (NIO ES6 *via* CATL<sup>40</sup>; **Table 1**). In fact, in spite of a much larger current market share of NCM than NCA, the competitiveness of high-Ni, low-Co NCM is not agreed upon among experts in the field (*e.g.*, AESC, BASF, CATL, LG Chem, Samsung SDI, SK Innovation, Umicore). By virtue of a similar effect of Al to that of Co on rate capability and its effective stabilization of the layered structure at low concentrations mentioned above, removing Co from NCA is relatively straightforward without notably compromising performance<sup>33</sup>. High-Ni, low-Co NCM, however, can suffer from (i) insufficient Co to enable desired rate capability, and/or (ii) insufficient Mn to ensure acceptable cycle and thermal stability. Further, in the absence of Al, more surface Li residues compromise chemical/electrochemical stability. As a result, doping (Al and more; see below) and surface conditioning are crucial<sup>24</sup>, which diminish its cost advantages over NCA. For some cathode manufacturers, 2019–2020 will mark a critical point for establishing product roadmaps prioritizing high-Ni, low-Co NCM *vs.* NCA for the coming decade.

**Non-standard chemistry.** Probably no elements are better than Co, Mn, and Al that make up for the instability of Ni. While elements such as magnesium, zirconium, and titanium are routinely introduced in commercial high-Ni layered oxides for performance tuning (lifetime, conductivity, *etc.*)<sup>24</sup>, optimal amounts are typically very small, sometimes down to ppm levels, as detriments often coincide with benefits (**Fig. 2k**). Large usage can give rise to substantial structural defects (*e.g.*, cation mixing), lattice distortion, and impurities, severely worsening electrochemical properties<sup>12</sup>. Synthesis is another constraint; as opposed to co-precipitation,

dopants are often coated onto precipitated materials and incorporated into final products during calcination<sup>41</sup>, and a large amount can result in notable compositional nonuniformity and performance inconsistency at industrial production. Commercial layered oxides doped with a variety of elements still as a rule adopt the standard nomenclature, *i.e.*, NCM/NCA. This will not be the case for some future generations with increasingly less Co, Mn, and/or Al, but more alternative dopants (*e.g.*, eLNO, Johnson Matthey<sup>42</sup>).

A recent revived interest in LiNiO<sub>2</sub> (LNO; up to 240–250 mAh g<sup>-1</sup> at 4.3 V<sub>Li</sub>)<sup>43</sup> opens up a fertile chemical playground for compositional designs of next-generation low-/zero-Co, ultrahigh-Ni layered oxides alternative to the standard NCM/NCA chemistry. To start with, simple designs based on well-established dopants, *e.g.*, Li[Ni<sub>1-x-y</sub>Mn<sub>x</sub>Al<sub>y</sub>]O<sub>2</sub> (NMA) and Li[Ni<sub>1-2x-y</sub>Ti<sub>x</sub>Mg<sub>x</sub>Al<sub>y</sub>]O<sub>2</sub> (NTMA), may prove to be attractive. Looking at a larger pool of elements reported in the literature (*e.g.*, Mo, Nb, Zr, B, Ta, W, Cr, Ga, Fe, Na)<sup>43,44</sup>, going back to the fundamentals (*e.g.*, stoichiometry, site occupancy, long-range ordering) is crucial to a strategic compositional design. For instance, dopant cations with an ionic radius (*e.g.*, Al<sup>3+</sup>, 0.535 Å) smaller than Ni<sup>3+</sup> (0.56 Å) tend to cluster, whereas larger cations promote the formation of rock-salt structures (*e.g.*, Ti<sup>4+</sup>, 0.605 Å; Zr<sup>4+</sup>, 0.72 Å; Nb<sup>5+</sup>, 0.64 Å; W<sup>6+</sup>, 0.60 Å) or substitute Li<sup>+</sup> in the lithium slabs (*e.g.*, Ni<sup>2+</sup>, 0.69 Å; Mg<sup>2+</sup>, 0.72 Å) depending on their valence states. Metal-oxygen bonds are strengthened by certain dopants (*e.g.*, Al, Ti, Nb, Zr, Ta, W, Cr) and weakened by others (*e.g.*, Zn). The tuned electronic structure, in turn, dictates electrochemical properties. It is worth noting that strictly Co-free compositions may not be necessary from purely economic or geopolitical standpoints as much as being a marketing tactic. Increasing mining and battery recycling will allow a modulated growth of demand for cobalt in the coming decade<sup>27</sup>.

So far, there is a lack of widely accepted theories governing dopant selection for LNO. Literature reports are mostly based on trial-and-error and sometimes arrive at dramatically conflicting assessments, often a result of structural ambiguities particularly at light doping (*e.g.*, < 2%). For example, the disordered rock-salt structure, generally dismissed because of poor Li-ion conductivity, recently demonstrated promise in doped LNO<sup>45</sup>. To guide a high-throughput screening of desired dopants, a robust understanding of the electronic structure of LNO and its derivatives should be a critical aspect of future investigation.

**Compositional heterogeneity?** One approach to boost the energy content while preserving cycle/thermal stability of layered oxides is through the use of compositional heterogeneity<sup>12</sup>. In a full concentration-gradient NCM particle, a continuous compositional change aims to hybridize the high energy from a Ni-enriched interior and high thermal stability from a Mn-enriched exterior. First reported in 2005<sup>47</sup>, this concept has been enhanced over the years in academic laboratories, with the energy and lifetime performance claimed to exceed standard NCM/NCA of similar Ni fraction<sup>12,13</sup>. Interestingly, in spite of continuing commercialization efforts<sup>48</sup>, concentration-gradient NCM has not registered a notable market share thus far in the cathode landscape for automotive batteries. This may be ascribed to several fundamental impediments to its large-scale production. Due to a more complicated co-precipitation, cost and performance consistency are concerns; calcination is another intrinsic challenge, since the Ni-rich core and Mn-rich surface require different heating temperatures to reach desired electrochemical properties (**Fig. 3b**)<sup>3,23,24</sup>. In addition, surface passivation may be necessary to suppress Mn dissolution<sup>49</sup>. To date, systematic analyses on these limitations are lacking in the literature, which will shed some light on the future prospect of a large industrial adoption of concentration-gradient NCM.

## Production and conditioning

Apart from chemistry, particle morphology, microstructure, and surface properties are central to optimal energy output of layered oxide cathodes. For automotive batteries, the volumetric aspect (*i.e.*, energy density, Wh l<sup>-1</sup>) is often more critical. In this respect, an electrode loading and density higher than 3–4 mAh cm<sup>-2</sup> and 3.0–3.4 g cm<sup>-3</sup>, respectively, of state-of-the-art high-Ni NCM/NCA electrodes<sup>13</sup> are desired. Meanwhile, material production plays a role in driving down costs. Here, we discuss current/emerging production methods for improving these metrics.

**Particle engineering.** Commercial Ni-based layered oxides produced by the standard co-precipitation route consist of spherical polycrystalline secondary particles densely packed by hundreds of primary particles. **Fig. 3a** illustrates the synthesis route with mixed transition-metal ions<sup>50</sup>. For high-Ni layered oxides (*e.g.*, NCM-811), the production processes are more complex and the facility must meet more stringent standards, compared to those with less Ni (*e.g.*, NCM-523)<sup>23,24</sup>. This includes modified co-precipitation, LiOH (instead of Li<sub>2</sub>CO<sub>3</sub>) as the Li source, longer, multistep calcination using flowing O<sub>2</sub>, mandatory post-calcination surface treatments, and vacuum/N<sub>2</sub> packaging; most equipment necessitates high corrosion resistance (LiOH and O<sub>2</sub>) and strict humidity control. Various parameters for co-precipitation and calcination (*e.g.*, pH, ammonia amount, heating temperature) need to be adjusted (**Fig. 3b**). For commercial NCMs, raw materials account for 75–90% of the total cost, of which cobalt makes up a significant portion (one example in **Fig. 3c**)<sup>3,24</sup>. Factoring in some extra costs in raw materials (LiOH) and calcination (*e.g.*, energy and O<sub>2</sub> gas), the total cost of NCM-811 per kWh comes nonetheless close to NCM-523 and much lower than NCM-111 owing to higher energy content and less Co usage. Barring a wild swing of metal price, further cost reduction will primarily be driven by increases in energy output. Savings can also come from improved

production in volume and efficiency (*e.g.*, yield and throughput rate)<sup>7</sup>, though the costs of production are already small relative to raw material costs. On the other hand, gross margins of profit on the part of cathode producers currently run higher for high-Ni NCM/NCA (10–30%) than low-Ni NCM (< 10%)<sup>3,24</sup>. As the market further matures, competition can drive down profit margins and lead to lower prices for cell manufacturers and OEMs. Better cost structures can also be achieved by in-house material production.

The particle morphology and microstructure of layered oxides are pivotal to a range of electrochemical properties (**Fig. 3d**). For starters, the size, shape of primary particles and their alignment within a secondary particle, as well as the electrode tortuosity influenced by secondary particles, dictate rate capability (Li-ion transport) and are relevant to extreme fast charging (XFC) capability of the battery<sup>51</sup>. The mechanical strength of aggregated secondary particles is critical as well to enable high electrode density without cracking during electrode pressing or battery operation. State-of-the-art high-Ni NCM/NCA can notably outperform LiCO<sub>2</sub> (LCO) in specific energy (Wh kg<sup>-1</sup>), but not energy density (Wh l<sup>-1</sup>), a result of lower electrode density (3.0–3.4 *w.* 3.8–4.2 g cm<sup>-3</sup>; **Fig. 1c**)<sup>13</sup>. With higher density ( $\geq 3.4$  g cm<sup>-3</sup>) and loading ( $\geq 4$  mAh cm<sup>-2</sup>), however, rate capability and operational lifetime are usually severely compromised due to high impedance, particle pulverization, and electrode delamination<sup>34,52</sup>. Worse, decreasing electrolyte wettability and larger operating currents lead to non-uniform Li utilization and irregular electrochemical reactions through the thick electrode, exacerbating mechanical degradation<sup>53</sup>.

The aforementioned limitations of standard polycrystalline secondary particles of layered oxides have fueled research on particle engineering. Tuning of the primary particles, such as nanosizing<sup>54</sup>, reshaping/realignment<sup>55</sup>, and grain boundary reinforcement<sup>54,56</sup> (Approach 3, 4, and 2, respectively, **Fig. 3e**), is believed to facilitate Li-ion transport, alleviate strains, and

increase mechanical strength of an aggregated secondary particle. Microstructural tuning is realized through modified calcination (*e.g.*, temperature, duration, Li/metal ratio) and post surface treatments (*e.g.*, coating). A more drastic approach is the single-crystal morphology<sup>57-59</sup>. Compared to polycrystalline particles, micron-scale single-crystal particles can be far more mechanically robust during electrode pressing and battery operation, despite inferior specific capacity and rate capability (Approach 5, **Fig. 3e**). The superior electrochemical stability may thus allow higher charging voltages (*e.g.*,  $\geq 4.5$  V<sub>Li</sub>) to compensate for specific capacity while retaining cycle and thermal stability<sup>57</sup>, provided that compatible electrolytes are developed.

The current generations of single-crystal Ni-based layered oxides still have a large room for optimization, including production cost, electrode density, and rate capability. The most economical synthesis route is a simple calcination of precipitated precursors with a smaller average particle size than the industrial norm (*e.g.*, 3–5 *vs.*  $\geq 10$   $\mu\text{m}$ ), at high temperatures (*e.g.*,  $\geq 950$  °C)<sup>57,58</sup> and/or with chemical reagents (*i.e.*, flux)<sup>59</sup>. However, the tuned co-precipitation and calcination processes decrease production throughput and lead to higher costs. Lately, industrial production is burgeoning, but mostly of low-Ni NCMs (*e.g.*, NCM-523); production of high-Ni NCM/NCA necessitates a stepwise calcination of increasing Li/metal ratios and decreasing temperatures<sup>13</sup>. Some complex synthesis routes can obtain single-crystal particles directly<sup>60</sup>, but are restricted by severe cost and scalability issues for large-scale production. To fully reap the benefits of the single-crystal morphology, a facile production with a robust control of particle size and distribution, structural defects, impurities, and surface Li residues will be the focus of future development.

**Surface stabilization.** As described above, the as-synthesized high-Ni layered oxide powder is routinely surface treated for enhanced stability during both electrode fabrication and cell operation. Besides particle mechanical degradation, the high surface reactivity with electrolyte

solutions causes severe gassing and deteriorates lifetime and safety of the battery (residual Li compounds<sup>22</sup> and singlet oxygen release at large Li utilization<sup>16</sup>). For industrial production, dry or water-based coating processes are the most economical. In the former case, coating precursors are mixed with and adhered onto the cathode material *via* mechanical or chemical interactions<sup>61</sup>. The water-based route washes off surface Li residues directly, while coating precursors are precipitated onto the cathode and form a more uniform coating upon solvent evaporation<sup>41,62</sup>. The water exposure, however, promotes surface rock-salt phase formation (Li leaching) and decreases specific capacity and cyclability. Alternatively, wet coating in organic solvents eschews this issue and offers desired coating uniformity<sup>41,62</sup>, though at extra cost involving fire hazards and waste disposal. The deposition/precipitation is followed by calcination, during which the coating precursors, sometimes through reacting with native species at the cathode surface, transform into the final coating layer.

The layered oxide can also be surface conditioned by gaseous species, such as chemical vapor deposition (CVD)<sup>63</sup> and atomic layer deposition (ALD)<sup>56,64</sup>. These systems provide the best uniformity, capable of self-terminating, sub-nanometer level thickness control. Recent advances of continuous ALD systems have dramatically lowered the price over conventional pulsed systems by increasing throughput *via* sample translation<sup>64</sup>. Nonetheless, these methods need to decrease further in price for large-scale implementation.

The broad array of coating materials may cover the aggregated secondary particles only, or they can sufficiently penetrate through and coat primary particles, often by solution- or gas-based treatments (**Fig. 3e**). Surface passivation at the primary particle level can be more effective at suppressing gas generation and mechanical fracture during cycling, as the filled inner voids/crevasses and tuned primary particle morphologies can reduce contact area with electrolytes and diffuse strains from anisotropic lattice distortion<sup>56</sup>. Cobalt can also be placed

strategically at crucial areas (*e.g.*, grain boundaries) despite a low bulk content<sup>54,61</sup>. Depending upon the efficacy and cost, future high-Ni layered cathodes will likely rely on a combination of the various particle engineering and surface stabilization techniques.

## **Outlook**

With low-cobalt NCA largely deployed and NCM-811 on track for full commercialization, high-nickel layered oxides are expected to preserve their supremacy in Li-based automotive batteries for passenger electric vehicles at least through the next decade. Contingent upon the anode (graphite-silicon or Li metal), next-generation layered cathodes will enable a cell-level specific energy of, respectively, 300–350 or 350–500 Wh kg<sup>-1</sup>, with a driving range  $\geq 600$  km from a single charge. A high Ni fraction, optionally coupled with extended operating voltages, will further drive up the energy output. Cobalt usage needs to drop substantially (*e.g.*,  $\leq 50$  g per kWh) to sustain a projected exponential growth of the global EV fleet. While NCA is eyeing a possible Co elimination, NCM will in the near future continue to use a larger fraction of Co for chemical/electrochemical stability. Nonetheless, the lines between NCM *vs.* NCA will increasingly blur as future ultrahigh-Ni layered oxides contain less Mn and Al for higher energy content, but more alternative dopants (*e.g.*, Mg, Zr, Ti, Mo, Cr) to address a series of intrinsic hurdles associated with large Li utilization and low Co usage. As such, we expect more non-standard compositional designs to make a meaningful contribution to the global EV market in the coming decade.

Energy enhancements will also come from electrode density and loading. High electrode density (*e.g.*,  $\geq 3.4$  g cm<sup>-3</sup>) is a great challenge, where state-of-the-art high-Ni NCM/NCA still fall short compared to LiCoO<sub>2</sub> for high energy density (Wh l<sup>-1</sup>). Particle engineering and surface conditioning, such as primary particle realignment, grain boundary strengthening, and single-crystal morphology, will confer various benefits to the mechanical durability of

the cathode material. Meanwhile, ultrahigh electrode loading (*e.g.*, 5–10 mAh cm<sup>-2</sup>) has been demonstrated *via* non-conventional electrode fabrication<sup>65,66</sup>. Since most stabilization strategies (compositional, morphological, or microstructural) impose a penalty in energy content at a given voltage, their effectiveness needs to be validated with caution. An in-depth mechanistic understanding will also lead to a purposeful combination for synergistic effects.

The driver for lower prices of high-Ni layered cathodes, besides higher energy content, will be further upscaling and efficiency enhancements of material production. Given the large financial investment committed to improving and expanding existing infrastructure, it will be difficult for emerging production methods to become cost-competitive compared to the co-precipitation route. On the other hand, more sophisticated add-on systems offering performance benefits may be adopted at lower prices (*e.g.*, primary particle surface coating). While little room is left for significant improvements, we expect more exciting opportunities on diverse development roadmaps of next-generation high-nickel layered oxide cathodes in a not-so-distant electrified future.

### **Acknowledgements**

The authors gratefully acknowledge the support from the Assistant Secretary for Energy Efficiency and Renewable Energy, Office of Vehicle Technologies of the U.S. Department of Energy through the award number DE-EE0008445 and the Welch Foundation F-1254.

### **Competing financial interests**

The authors declare no competing financial interests.

## References

1. Irle, R. Global EV Sales for 2018 – Final Results. *EV-volumes.com* (Trollhättan, Sweden, 2019).
2. Global EV Outlook 2019. (International Energy Agency, Paris, France, 2019).
3. The Push to High Nickel Content in Layered Oxides – Production, Cost, and Supply & Demand (in Chinese). (Shanxi Securities, China, 2019).
4. Alvarez, S. Tesla Model 3 Battery Details Revealed in Partial Teardown and Analysis. *Teslarati* (17 May 2018).
5. Goldie-Scot, L. A Behind the Scenes Take on Lithium-Ion Battery Prices. (Bloomberg New Energy Finance, 2019).
6. U.S. DRIVE Electrochemical Energy Storage Technical Team Roadmap. (U.S. Council for Automotive Research, 2017).
7. Schmuch, R., Wagner, R., Hörpel, G., Placke, T. & Winter, M. Performance and Cost of Materials for Lithium-based Rechargeable Automotive Batteries. *Nat. Energy* **3**, 267-278 (2018).
8. Kwade, A. et al. Current Status and Challenges for Automotive Battery Production Technologies. *Nat. Energy* **3**, 290-300 (2018).
9. Fang, Q. NCM/NCA vs. LFP: the Competitive Edge of LFP (in Chinese). *China Battery Enterprise Alliance* (14 March 2019).
10. China's Installed Battery Capacity Surges to 56.9 GWh. *InsideEVs* (22 Jan 2019).
11. Pillot, C. Lithium Ion Battery Raw Materials Supply and Demand 2016-2025. *AABC Europe* (Avicenne Energy, Mainz, Germany, 2017).
12. Myung, S.-T. et al. Nickel-Rich Layered Cathode Materials for Automotive Lithium-Ion Batteries: Achievements and Perspectives. *ACS Energy Lett.* **2**, 196-223 (2017).
13. Kim, J. et al. Prospect and Reality of Ni-Rich Cathode for Commercialization. *Adv. Energy Mater.* **8**, 1702028 (2018).
14. Mineral Commodity Summaries 2018 (U.S. Geological Survey, 2018).
15. Li, W., Yaghoobnejad Asl, H., Xie, Q. & Manthiram, A. Collapse of  $\text{LiNi}_{1-x-y}\text{Co}_x\text{Mn}_y\text{O}_2$  Lattice at Deep Charge Irrespective of Ni Content in Lithium-Ion Batteries. *J. Am. Chem. Soc.* **141**, 5097-5101 (2019).
16. Wandt, J., Freiberg, A. T. S., Ogorodnik, A. & Gasteiger, H. A. Singlet Oxygen Evolution from Layered Transition Metal Oxide Cathode Materials and Its Implications for Lithium-Ion Batteries. *Mater. Today* **21**, 825-833 (2018).
17. Gilbert, J. A., Shkrob, I. A. & Abraham, D. P. Transition Metal Dissolution, Ion Migration, Electrocatalytic Reduction and Capacity Loss in Lithium-Ion Full Cells. *J. Electrochem. Soc.* **164**, A389-A399 (2017).
18. Lin, F. et al. Surface Reconstruction and Chemical Evolution of Stoichiometric Layered Cathode Materials for Lithium-Ion Batteries. *Nat. Commun.* **5**, 3529 (2014).
19. Ma, L., Nie, M., Xia, J. & Dahn, J. R. A Systematic Study on the Reactivity of Different Grades of Charged  $\text{Li}[\text{Ni}_x\text{Mn}_y\text{Co}_z]\text{O}_2$  with Electrolyte at Elevated Temperatures Using Accelerating Rate Calorimetry. *J. Power Sources* **327**, 145-150 (2016).
20. Ohzuku, T., Ueda, A. & Nagayama, M. Electrochemistry and Structural Chemistry of  $\text{LiNiO}_2$  ( $R\bar{3}m$ ) for 4 Volt Secondary Lithium Cells. *J. Electrochem. Soc.* **140**, 1862-1870 (1993).
21. You, Y., Celio, H., Li, J., Dolocan, A. & Manthiram, A. Modified High-Nickel Cathodes with Stable Surface Chemistry Against Ambient Air for Lithium-Ion Batteries. *Angew. Chem. Int. Ed.* **57**, 6480-6485 (2018).

22. Renfrew, S. E. & McCloskey, B. D. Residual Lithium Carbonate Predominantly Accounts for First Cycle CO<sub>2</sub> and CO Outgassing of Li-Stoichiometric and Li-Rich Layered Transition-Metal Oxides. *J. Am. Chem. Soc.* **139**, 17853-17860 (2017).
23. Yakovleva, M. From Raw Material to Next Generation Advanced Batteries. (FMC Corporation, 2017).
24. Production and Cost Analysis of Nickel-Rich Layered Cathode Materials (in Chinese). (CITIC Securities, China, 2018).
25. Panasonic Starts Mass-Production of High-Capacity 3.1 Ah Lithium-Ion Battery. *Panasonic Newsroom Global* (18 Dec 2009).
26. Jeong, M. H., Lee, J. H. & Jung, S. H. Electrolyte for Lithium Secondary Battery and Lithium Secondary Battery Comprising Same. *U.S. Patent 20,180,183,100 A1* (Soulbrain Co. Ltd., 2018).
27. Price Elasticity of Supply for Cathode Materials in A Fast-Growing Vehicle Electrification Scenario. *AABC Europe* (Umicore, Strasbourg, France, 2019).
28. Fiscal Year 2018 Advanced Vehicle Technologies Research Funding Opportunity Announcement (FOA): 1a. Developing Low-Cobalt Active Cathode Materials for Next-Generation Li-Ion Batteries. *DOE DE-FOA-0001919*. (U.S. DOE, 2018).
29. Delmas, C., Saadoun, I. & Rougier, A. Proceedings of the 6th International Meeting on Lithium Batteries: The Cycling Properties of the Li<sub>x</sub>Ni<sub>1-y</sub>Co<sub>y</sub>O<sub>2</sub> Electrode. *J. Power Sources* **44**, 595-602 (1993).
30. Ohzuku, T., Ueda, A. & Kouguchi, M. Synthesis and Characterization of LiAl<sub>1/4</sub>Ni<sub>3/4</sub>O<sub>2</sub> (R $\bar{3}$ m) for Lithium-Ion (Shuttlecock) Batteries. *J. Electrochem. Soc.* **142**, 4033-4039 (1995).
31. Guilnard, M., Rougier, A., Grüne, M., Croguennec, L. & Delmas, C. Effects of Aluminum on the Structural and Electrochemical Properties of LiNiO<sub>2</sub>. *J. Power Sources* **115**, 305-314 (2003).
32. Arai, H., Okada, S., Sakurai, Y. & Yamaki, J. Electrochemical and Thermal Behavior of LiNi<sub>1-x</sub>M<sub>x</sub>O<sub>2</sub> (M = Co, Mn, Ti). *J. Electrochem. Soc.* **144**, 3117-3125 (1997).
33. Li, H. et al. Is Cobalt Needed in Ni-Rich Positive Electrode Materials for Lithium Ion Batteries? *J. Electrochem. Soc.* **166**, A429-A439 (2019).
34. Watanabe, S., Kinoshita, M., Hosokawa, T., Morigaki, K. & Nakura, K. Capacity Fading of LiAl<sub>y</sub>Ni<sub>1-x-y</sub>Co<sub>x</sub>O<sub>2</sub> Cathode for Lithium-Ion Batteries during Accelerated Calendar and Cycle Life Tests (Effect of Depth of Discharge in Charge-Discharge Cycling on the Suppression of the Micro-Crack Generation of LiAl<sub>y</sub>Ni<sub>1-x-y</sub>Co<sub>x</sub>O<sub>2</sub> Particle). *J. Power Sources* **260**, 50-56 (2014).
35. Li, W. et al. Mn versus Al in Layered Oxide Cathodes in Lithium-Ion Batteries: A Comprehensive Evaluation on Long-Term Cyclability. *Adv. Energy Mater.* **8**, 1703154 (2018).
36. Madhavi, S., Subba Rao, G. V., Chowdari, B. V. R. & Li, S. F. Y. Effect of Aluminium Doping on Cathodic Behaviour of LiNi<sub>0.7</sub>Co<sub>0.3</sub>O<sub>2</sub>. *J. Power Sources* **93**, 156-162 (2001).
37. Rossen, E., Jones, C. D. W. & Dahn, J. R. Structure and Electrochemistry of Li<sub>x</sub>Mn<sub>y</sub>Ni<sub>1-y</sub>O<sub>2</sub>. *Solid State Ionics* **57**, 311-318 (1992).
38. Seiwert, M. VW's Batteries Contain Four Times as much Cobalt as Tesla Batteries (in German). *WirtschaftsWoche* (29 March 2019).
39. Fortuna, C. Cobalt-Free Car Batteries In the Works for Panasonic & Tesla. *Clean Technica* (9 June 2018).
40. Lima, P. NIO Begins Deliveries of ES6 with NCM 811 Battery. *PushEVs* (20 June 2019).
41. Son, Y. S. & Hong, J. Method of Fabricating Cathode Active Material of Lithium Secondary Battery. *U.S. Patent 20,180,034,050 A1* (Laminar Co. Ltd., Samsung Electronics Co. Ltd. & Samsung SDI Co. Ltd., 2018).
42. Johnson Matthey Achieves Two Major Milestones in Journey to Commercialise eLNO. *JM News* (28 March 2019).

43. Bianchini, M., Roca-Ayats, M., Hartmann, P., Brezesinski, T. & Janek, J. There and Back Again – The Journey of LiNiO<sub>2</sub> as a Cathode Active Material. *Angew. Chem. Int. Ed.* **58**, 2-27 (2019).
44. Weigel, T. et al. Structural and Electrochemical Aspects of LiNi<sub>0.8</sub>Co<sub>0.1</sub>Mn<sub>0.1</sub>O<sub>2</sub> Cathode Materials Doped by Various Cations. *ACS Energy Lett.* **4**, 508-516 (2019).
45. Kim, U.-H. et al. Pushing the Limit of Layered Transition Metal Oxide Cathodes for High-Energy Density Rechargeable Li Ion Batteries. *Energy Environ. Sci.* **11**, 1271-1279 (2018).
46. Turcheniuk, K., Bondarev, D., Singhal, V. & Yushin, G. Ten Years Left to Redesign Lithium-Ion Batteries. *Nature* **31**, 467-470 (2018).
47. Sun, Y.-K., Myung, S.-T., Kim, M.-H., Prakash, J. & Amine, K. Synthesis and Characterization of Li[(Ni<sub>0.8</sub>Co<sub>0.1</sub>Mn<sub>0.1</sub>)<sub>0.8</sub>(Ni<sub>0.5</sub>Mn<sub>0.5</sub>)<sub>0.2</sub>]O<sub>2</sub> with the Microscale Core-Shell Structure as the Positive Electrode Material for Lithium Batteries. *J. Am. Chem. Soc.* **127**, 13411-13418 (2005).
48. Fiscal Year 1983 - 2019 SBIR/STTR Awards. (U.S. Small Business Administration, 2019).
49. Li, W., Kim, U.-H., Dolocan, A., Sun, Y.-K. & Manthiram, A. Formation and Inhibition of Metallic Lithium Microstructures in Lithium Batteries Driven by Chemical Crossover. *ACS Nano* **11**, 5853-5863 (2017).
50. Toya, H. N. et al. Nickel-Cobalt-Manganese Complex Hydroxide Particles and Method for Producing Same, Positive Electrode Active Material for Nonaqueous Electrolyte Secondary Battery and Method for Producing Same, and Nonaqueous Electrolyte Secondary Battery. *U.S. Patent 20,120,270,107 A1* (Sumitomo Metal Mining Co. Ltd. & Toyota Motor Corp., 2012).
51. Liu, Y., Zhu, Y. & Cui, Y. Challenges and Opportunities towards Fast-Charging Battery Materials. *Nat. Energy* **4**, 540-550 (2019).
52. Muto, S. et al. Capacity-Fading Mechanisms of LiNiO<sub>2</sub>-Based Lithium-Ion Batteries: II. Diagnostic Analysis by Electron Microscopy and Spectroscopy. *J. Electrochem. Soc.* **156**, A371-A377 (2009).
53. Oriksa, Y. et al. Ionic Conduction in Lithium Ion Battery Composite Electrode Governs Cross-Sectional Reaction Distribution. *Sci. Rep.* **6**, 26382 (2016).
54. Pullen, A., Rempel, J. & Sriramulu, S. Polycrystalline Layered Metal Oxides Comprising Nano-Crystals. *U.S. Patent 20,190,140,276 A1* (CAMX Power LLC, 2019).
55. Kim, J. et al. Nickel-based Active Material for Lithium Secondary Battery, Method of Preparing the Same, and Lithium Secondary Battery Including Positive Electrode Including the Nickel-based Active Material. *U.S. Patent 20,180,026,268 A1* (Samsung SDI Co. Ltd., 2018).
56. Yan, P. et al. Tailoring Grain Boundary Structures and Chemistry of Ni-Rich Layered Cathodes for Enhanced Cycle Stability of Lithium-Ion Batteries. *Nat. Energy* **3**, 600-605 (2018).
57. Li, J. et al. Comparison of Single Crystal and Polycrystalline LiNi<sub>0.5</sub>Mn<sub>0.3</sub>Co<sub>0.2</sub>O<sub>2</sub> Positive Electrode Materials for High Voltage Li-Ion Cells. *J. Electrochem. Soc.* **164**, A1534-A1544 (2017).
58. Park, S., Chang, S. K., Park, H.-K., Hong, S. T. & Choi, Y. Electrode Active Material for Lithium Secondary Battery. *U.S. Patent 20,140,356,719 A1* (LG Chem Ltd., 2014).
59. Kimijima, T., Zettsu, N. & Teshima, K. Growth Manner of Octahedral-Shaped Li(Ni<sub>1/3</sub>Co<sub>1/3</sub>Mn<sub>1/3</sub>)O<sub>2</sub> Single Crystals in Molten Na<sub>2</sub>SO<sub>4</sub>. *Cryst. Growth Des.* **16**, 2618-2623 (2016).
60. Han, X., Meng, Q., Sun, T. & Sun, J. Preparation and Electrochemical Characterization of Single-Crystalline Spherical LiNi<sub>1/3</sub>Co<sub>1/3</sub>Mn<sub>1/3</sub>O<sub>2</sub> Powders Cathode Material for Li-Ion Batteries. *J. Power Sources* **195**, 3047-3052 (2010).
61. Kim, J. et al. A Highly Stabilized Nickel-Rich Cathode Material by Nanoscale Epitaxy Control for High-Energy Lithium-Ion Batteries. *Energy Environ. Sci.* **11**, 1449-1459 (2018).
62. Myung, S.-T. et al. Role of Alumina Coating on Li-Ni-Co-Mn-O Particles as Positive Electrode Material for Lithium-Ion Batteries. *Chem. Mater.* **17**, 3695-3704 (2005).

63. Son, I. H., Park, J. H., Kwon, S., Mun, J. & Choi, J. W. Self-Terminated Artificial SEI Layer for Nickel-Rich Layered Cathode Material *via* Mixed Gas Chemical Vapor Deposition. *Chem. Mater.* **27**, 7370-7379 (2015).
64. Maydannik, P. S., Kaariainen, T. O. & Cameron, D. C. Continuous Atomic Layer Deposition: Explanation for Anomalous Growth Rate Effects. *J. Vac. Sci. Technol. A* **30**, 01A122 (2011).
65. Duong, H. M., Feigenbaum, H. & Hong, J. Dry Energy Storage Device Electrode and Methods of Making the Same. *U.S. Patent, 20,150,303,481 A1* (Maxwell Technologies Inc., 2015).
66. Chiang, Y.-M., Duduta, M., Holman, R., Limthongkul, P. & Tan, T. Semi-Solid Electrodes Having High Rate Capability. *U.S. Patent 20,140,170,524 A1* (24M Technologies Inc., 2014).

**Table 1. A comparison of the estimated driving performance between some latest ICE vehicles and BEVs in varying price ranges**

Price* (US\$)	ICE vehicles				BEVs			
	OEM and model (2019)	Fuel tank capacity (l)	Fuel economy** (l/100 km)	Driving range (km)	OEM and model (2019)	Cathode chemistry	Battery pack size (kWh)	Driving range† (km)
< 20,000	Ford Fiesta SE	47	7.7	611				
	Toyota Yaris LE	44	6.6	636	BAIC EC220	LFP	unknown	206‡
	Fiat 500 Hatchback	40	7.8	511				
	Kia Forte LXS	53	6.8	777	JMC E200L	NCM	29.2	252‡
20,000 – 30,000	Honda Civic SE	47	6.4	728	Mitsubishi i-MiEV	LMO-NCM	16	100
	Toyota Camry SE	58	7.1	806	Roewe Ei5	NCM	52.5	420‡
	Nissan Rogue SV	55	8.1	680	Smart EQ Fortwo	LMO-NCM	17.6	93
	VW Golf 1.4T SE	50	7.2	693	BYD Yuan EV535	NCM	53.2	410‡
	Mazda CX-5 Touring	57	8.8	649	BAIC EU5 R550	NCM	60.2	460‡
30,000 – 40,000	Volvo S60 T5	58	8.0	719	Renault Zoe 50	NCM	52	390 <sup>l</sup>
	Subaru Outback 3.6R	70	10.2	689	VW e-Golf SEL	NCM	35.8	201
	Mercedes-Benz A-Class A 220	49	8.1	606	Nissan Leaf S Plus	NCM	62	364
	Ram 1500 Big Horn	93	11.1	838	Chevrolet Bolt LT	NCM	60	383
	VW Tiguan SEL	60	9.4	644	BYD Qin Pro EV	NCM	69.5	520‡
	Ford F-150 Super Cab XL	87	10.4	840	Hyundai Kona Electric SEL	NCM	64	415
40,000 – 60,000	BMW 3 series	59	8.1	734	BYD e6 (2017)	LFP	82	400 <sup>l</sup>
	Lexus RX 350	73	10.2	715	BMW i3 Basic	NCM	42.2	246

	Cadillac XT5 Basic	78	11.1	701	NIO ES6 Standard	NCM	84	490#
	Mercedes-Benz C-Class C 300	66	8.7	755	Tesla 3 Long Range	NCA	~75	500
60,000 – 100,000	Audi S7 3.0 TFSI	73	9.8	750	Jaguar I-Pace SE	NCM	90	377
	Porsche Cayenne	90	11.3	793	Audi e-tron Prestige	NCM	95	328
	BMW X5 xDrive50i	83	12.2	678	Tesla S Long Range	NCA	~100	595
	Maserati Levante S GranSport	80	13.3	601	Tesla X Long Range	NCA	~100	525

\*without subsidies and before tax

\*\*a weighted average of City and Highway fuel economy values (City, 55%; Highway, 45%) rated by the U.S. EPA (Environmental Protection Agency).

†Unless otherwise specified, driving range is rated by the U.S. EPA. Exceptions are marked by ‡ (NEDC, New European Driving Cycle), || (WLTP, Worldwide Harmonized Light Vehicle Test Procedure), or ¶ (unspecified), which generally yield more favorable results compared to the EPA rating.

NCM,  $\text{Li}[\text{Ni}_{1-x-y}\text{Co}_x\text{Mn}_y]\text{O}_2$ ; NCA,  $\text{Li}[\text{Ni}_{1-x-y}\text{Co}_x\text{Al}_y]\text{O}_2$ ; LMO,  $\text{LiMn}_2\text{O}_4$ ; LFP,  $\text{LiFePO}_4$ ; OEM, original equipment manufacturer.

**Table 2. A comparison between two extreme cases for layered oxides to reach 800 Wh kg<sup>-1</sup> at the material level**

Properties	‘Ultrahigh Nickel’	‘Ultrahigh Voltage’
Specific energy (Wh kg <sup>-1</sup> )	≥ 800	≥ 800
Nickel content (%)	≥ 90	≤ 50
Charging voltage vs. Li (V)	4.2–4.35	4.6–5.0
Lifetime (deep cycles)	< 500	N.A.*
Energy efficiency (%)	≥ 97	90–95
Rate capability (%)	~90	~85
Electrode density (g cm <sup>-3</sup> )	≤ 3.3	≤ 3.6
Thermal stability†	Very poor	Poor
Synthesis and conditioning‡	Complex	Simple
Air storage†	Unstable	Stable
Supply risk†	Medium (Ni, Li)	High (Co)

\*in need of stable ‘5-V’ electrolytes

See † **Fig. 2** and ‡ **Fig. 3** for more details

All electrochemical properties are obtained at 25 °C. Energy efficiency is measured at 1C rate. Rate capability refers to the capacity ratio measured between 1C and C/10 rates.

**Fig. 1 Lithium-ion batteries for the automotive market and cathode material landscape.**

**a**, Cumulative EV deployment estimated from recent OEMs declarations compared with the EV stock projection in two scenarios: cautious (‘New Policies Scenario’) and ambitious (‘EV30@30 scenario’)<sup>2</sup>. The announcements from OEMs include targeted sales in either absolute value or percentage, and models rollout. The ‘New Policies Scenario’ considers existing and announced policies that facilitate the EV adoption and charging infrastructure expansion. The ‘EV30@30’ scenario refers to the EV30@30 Campaign Declaration from the Electric Vehicle Initiative (EVI), *i.e.*, a 30% market share of EVs by 2030. **b**, A breakdown of production/material costs and mass of a typical LIB cell. Cell housing materials also include electrode current collectors. **c**, The specific energy and energy density for a series of fully or partially commercialized, next-generation, and ‘emerging’ cathodes for LIBs, calculated based on their specific capacity ( $\text{mA h g}^{-1}$ ), average discharge potential ( $V$  *vs.*  $\text{Li/Li}^+$ ,  $V_{\text{Li}}$ ), and electrode density ( $\text{g cm}^{-3}$ ). LCO,  $\text{LiCoO}_2$ ; NCM-*abc*,  $\text{Li}[\text{Ni}_a\text{Co}_b\text{Mn}_c]\text{O}_2$  ( $a+b+c = 1$ ); NCA-80,  $\text{Li}[\text{Ni}_{0.80}\text{Co}_{0.15}\text{Al}_{0.05}]\text{O}_2$ ; Ultrahigh Ni,  $\text{Li}[\text{Ni}_{1-\xi}\text{M}_{\xi}]\text{O}_2$  ( $\xi \leq 0.1$ , M = metal); LMO,  $\text{LiMn}_2\text{O}_4$ ; LFP,  $\text{LiFePO}_4$ ; LNMO,  $\text{LiNi}_{0.5}\text{Mn}_{1.5}\text{O}_4$ ; LMR,  $\text{Li}_{1+n}\text{M}_{1-n}\text{O}_2$ ; HV, high-voltage. ‘Emerging’ cathodes (*e.g.*, LMR, LNMO) still await fundamental advances in material development and/or other cell parts (*e.g.*, electrolytes, separators) and will not contribute meaningfully to the EV market until the late 2020s at the earliest. **d**, A hierarchal breakdown of specific energy from the pack to material level of LIBs. Error bars come from varying cell and battery design conditions, such as cathode composition, porosity, and thickness; anode type; cell type, stacking, and size; and battery packing efficiency. **e**, Supply (2018) and projected demand (2025) of lithium, nickel and cobalt per annum for various applications, with those for batteries highlighted. Panel adapted from: **a**. ref. 2 (International Energy Agency); **b**. ref. 8 (NPG) and internal results; **d**. ref. 12 (ACS) and internal results; **e**. ref. 27 (AABC Europe).

**Fig. 2 Compositional design principles of high-energy, low-cobalt layered oxides.** **a-c**, Charge-discharge profiles of (a) NCM-111 (charged to 4.4 V<sub>Li</sub>), (b) NCM-900505 (to 4.4 V<sub>Li</sub>) and (c) NCM-111 (to 5.0 V<sub>Li</sub>), showing a conventional nickel-based layered cathode and two polar extremes to boost its energy content: ultrahigh Ni content or upper cut-off voltages. The dashed line (upper right) illustrates a combination of these two approaches to varying degrees for higher energy output. **d-h**, A series of intrinsic issues causing severely compromised cell lifetime and safety<sup>15-19</sup>, which occur at large Li utilization irrespective of Ni fraction or charging voltages: from a clockwise direction, (d) poor thermal-abuse tolerance, (e) release of singlet oxygen, (f) dissolution of transition-metal ions, (g) surface structural reconstruction from the layered to a rock-salt phase, and (h) anisotropic lattice collapse along the crystallographic *c*-axis. **i**, unique challenges of high upper cut-off voltages: anodic decomposition of aprotic carbonate-based electrolytes and a high supply risk of cobalt<sup>11,14,27</sup>. **j**, unique challenges of high Ni content in cathode formulations: not fully reversible, multistep two-phase reactions during (de)lithiation<sup>20</sup> and accumulation of surface residual Li compounds (*i.e.*, hydroxides, carbonates)<sup>21,22</sup>. **k**, a comparison among a variety of dopants established at industrial production (*i.e.*, Co, Mn, Al, Mg, Zr, Ti, and more) in property tuning, costs, and ease of synthesis<sup>13,23,24,43</sup>. Panel adapted from: **e**. singlet O<sub>2</sub> evolution, ref. 16 (Elsevier); **h**. lattice variation, ref. 15 (ACS); **i**. prices *vs.* supply of metals used in LIBs, ref. 46 (NPG). All other panels use internal results.

**Fig. 3 Production and conditioning processes for high-energy, low-cobalt layered oxides.** **a**, Schematic illustration of industrial synthesis of nickel-based layered oxides<sup>50</sup>, showing unique challenges and requirements for high-Ni compositions during each step<sup>24</sup>. **b**, Variations of pH and ammonia concentration during metal co-precipitation and heating temperature during lithiation calcination as a function of Ni content in NCM materials (internal results). **c**, A cost breakdown per kWh of a series of fully or partially commercialized NCMs, including raw materials (Li<sub>2</sub>CO<sub>3</sub>

or  $\text{LiOH}\cdot\text{H}_2\text{O}$ ,  $\text{NiSO}_4\cdot 6\text{H}_2\text{O}$ ,  $\text{CoSO}_4\cdot 7\text{H}_2\text{O}$  and  $\text{MnSO}_4\cdot\text{H}_2\text{O}$ ) as well as production during co-precipitation and calcination (*i.e.*, energy, water,  $\text{NaOH}$ ,  $\text{NH}_4\cdot\text{H}_2\text{O}$ ,  $\text{N}_2/\text{O}_2$  gas, direct labor, equipment depreciation, waste disposal, and other costs)<sup>3,24</sup>. The prices of  $\text{Li}_2\text{CO}_3$ ,  $\text{LiOH}\cdot\text{H}_2\text{O}$ ,  $\text{NiSO}_4\cdot 6\text{H}_2\text{O}$ ,  $\text{CoSO}_4\cdot 7\text{H}_2\text{O}$ , and  $\text{MnSO}_4\cdot\text{H}_2\text{O}$  are, respectively, 12.4, 16.9, 3.5, 12.9, and 0.8 US\$  $\text{kg}^{-1}$  (as of August 2018). **d**, Practical challenges severely compromising lifetime and rate capability with high electrode density and loading<sup>34,52,53</sup>, including poor electrolyte wettability, particle pulverization, electrode delamination, *etc.* **e**, Established/emerging material stabilization techniques: Approach 1, surface coating of secondary particles<sup>41,62</sup>; Approach 2, grain boundary strengthening among primary particles<sup>54,56</sup>; Approach 3, primary particle nanosizing<sup>54</sup>; Approach 4, reshaping/realignment of primary particles<sup>55</sup>; Approach 5, single-crystal particles<sup>57-59</sup>. Panel adapted from: **c**. ref. 24 (CITIC Securities). All other panels use internal results.

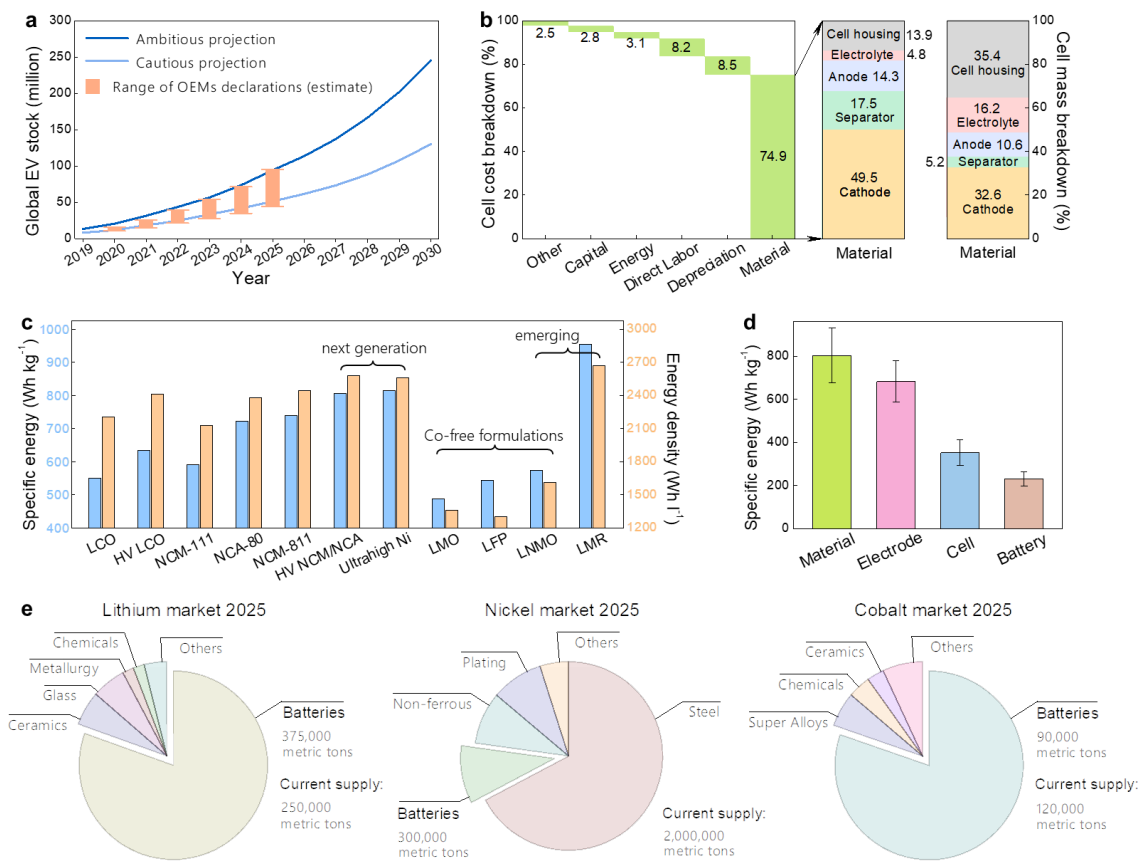


Figure 1

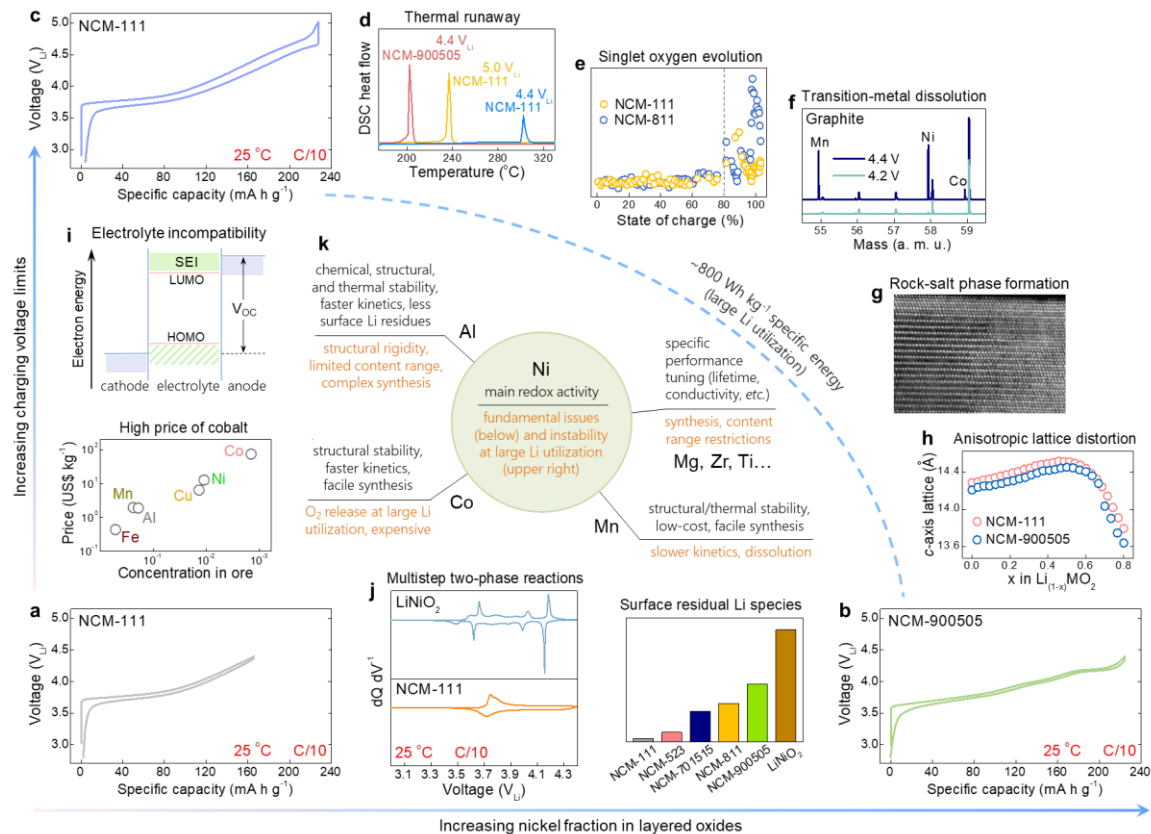


Figure 2

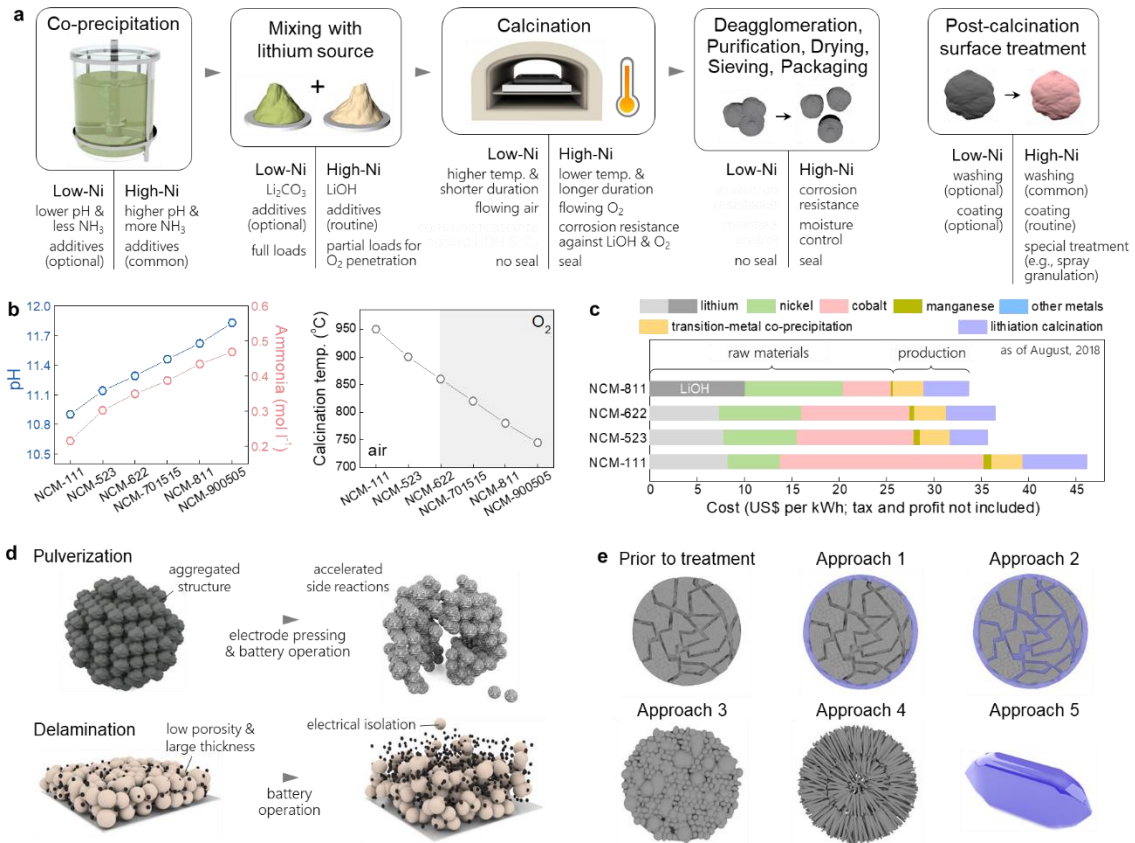


Figure 3